

# Self-Similar Relaxation Behavior at the Gel Point of a Blend of a Cross-Linking Poly( $\epsilon$ -caprolactone) Diol with a Poly(styrene-*co*-acrylonitrile)

Akihiro Izuka and H. Henning Winter\*

Chemical Engineering Department, University of Massachusetts,  
Amherst, Massachusetts 01003

Takeji Hashimoto

Department of Polymer Chemistry, Faculty of Engineering, Kyoto University,  
Kyoto 606, Japan

Received November 4, 1996; Revised Manuscript Received June 3, 1997<sup>®</sup>

**ABSTRACT:** Novel polymer properties can be achieved by blending high molecular weight linear chains into a cross-linking system of short linear chains. This study is concerned with the rheological properties that are dominated at first by the highly entangled linear chains. However, with increasing extent of cross-linking, the short chains connect into a network structure and begin to dominate the rheology. The material here consists of cross-linking poly( $\epsilon$ -caprolactone) diol (PCL) and up to 40% of linear poly(styrene-*co*-acrylonitrile) (SAN) of high molecular weight. The blend was molecularly mixed before cross-linking. Three competing processes determine the structure of the system, (1) chemical cross-linking of the low molecular weight species into a sample spanning network of interpenetrating chains, (2) fluctuations in composition due to phase separation at increasing extents of reaction, and (3) crystallization of the PCL, which we tried to suppress as much as possible. At the gel point, systems with low SAN content show the typical scaling behavior of the critical gel with a self-similar relaxation spectrum,  $H(\lambda) = G_0/\Gamma(n) (\lambda/\lambda_0)^{-n}$ ,  $\lambda > \lambda_0$ , at low probing frequencies,  $\omega < 1/\lambda_0$ . However, for the systems with high concentrations of the inert component, the self-similar region did not develop, possibly due to the phase separation induced by the cross-linking. The relaxation exponent,  $n$ , decreased with increasing concentration of the highly entangled linear component. The results suggest that dynamic mechanical methods are applicable for determination of the gel point for homogeneous semi-IPN systems.

## Introduction

Interpenetrating polymer networks (IPNs)<sup>1</sup> have the potential for achieving a wide range of synergistic chemical and physical properties as required in specific polymer applications. IPNs are polymer blends in which the molecules of each component are cross-linked while being molecularly mixed with the other component(s). This is a unique way of conserving miscibility in temperature ranges in which the blend would otherwise phase separate. A semi-IPN is a special type of IPN comprising one cross-linkable polymer and a second nonreacting component of high molecular weight above its entanglement limit. Especially intriguing as novel materials are highly asymmetric semi-IPNs in which the inert polymer consists of highly entangled macromolecules and the cross-linking molecules are very small initially. At the gel point (GP) of such a system one would expect good adhesion and damping properties from the developing network and good cohesion from the entangled chains. These properties could, for instance, be useful for an adhesive layer in composite materials. In another application, a small amount of high molecular weight polymer could be added to a low molecular weight cross-linking system (which by itself would cross-link into a brittle solid) with the purpose of decreasing the brittleness of the fully cross-linked material.

The preparation of an IPN is a challenging task because it involves two different transition phenomena that may interfere with each other, i.e., liquid–liquid phase separation between the components and sol–gel transition of at least one of the components. Recent

experimental<sup>2–4</sup> and theoretical<sup>5,6</sup> studies specifically investigated the liquid–liquid phase separation process in semi-IPN systems. From these, it is widely understood that cross-linking may not only induce phase separation but also affect its kinetics. In order to control the final molecular structure, it is essential to understand the cross-linking behavior in greater detail.

Although numerous studies of IPNs were reported in the literature, most of them focused their efforts on the analysis of final properties and/or structures and less on the structure development. This study has the objective of determining the state of the sample at the sol–gel transition point, the so-called gel point, which is an important reference state for the development of new IPNs. The chemical gel point (GP) is defined as the instant at which the weight average molecular weight of the cross-linking component diverges to infinity. This may be detected chemically or physically. Beyond GP, the entire sample behaves as a solid even if only one of the components has solidified while the other component(s) is (are) still in the liquid state. In a multicomponent system such as an IPN, the presence of a second component might disturb the precise determination of GP in a yet unknown way.

Holly et al.<sup>7</sup> developed a simple rheological method to determine GP. It is based on the observation that materials at GP (called “critical gels” [CG]) exhibit a self-similar relaxation time spectrum (CW-spectrum)<sup>8–10</sup>

$$H(\lambda) = S/\Gamma(n)\lambda^{-n}, \quad \text{for } \lambda_0 < \lambda < \infty \quad (1)$$

which results in a relaxation modulus

<sup>®</sup> Abstract published in *Advance ACS Abstracts*, August 1, 1997.

$$G(t) = St^{-n} \quad \text{for } \lambda_0 < t < \infty \quad (2)$$

The gel stiffness,  $S$ , and the relaxation exponent,  $n$ , are the only material parameters necessary to completely characterize the linear viscoelastic properties at GP.  $\lambda_0$  indicates the crossover from the universal self-similar behavior to some material specific short-time behavior.

The same scaling behavior is also apparent in dynamic mechanical experiments on critical gels where the storage modulus,  $G'$ , and the loss modulus,  $G''$ , are

$$G' = \frac{G''}{\tan \delta_c} = S\omega^n \Gamma(1-n) \cos \delta_c \quad 0 < \omega < 1/\lambda_0 \quad (3)$$

The phase angle between stress and strain,  $\delta_c$ , is independent of frequency,  $\omega$ , but proportional to the relaxation exponent<sup>9</sup>

$$\delta_c = n\pi/2 \quad (4)$$

Holly et al.<sup>7</sup> probed the loss tangent of cross-linking polymers at a range of frequencies and identified GP as the instant at which eq 4 is satisfied, i.e.,  $\tan \delta$  curves intersect at GP.

Several studies explored this phenomenon and determined  $S$  and  $n$  values for single-component systems including poly(dimethylsiloxane) (PDMS),<sup>8-11</sup> polyurethanes,<sup>12-16</sup> epoxy systems,<sup>17</sup> poly(oxypropylene),<sup>18</sup> and even physically cross-linked polymers.<sup>19,20</sup> The low-frequency self-similar behavior was observed in all these systems. The values of  $n$  varied over about the entire range between 0 and 1, depending on molecular compositions and cross-linking conditions. Short chains seem to give values of  $n$  around 0.7, while long chains form critical gels with  $n$  around 0.5.<sup>21</sup>

Since the self-similar behavior of CG is universally observed in many different systems, it is expected to also occur in an IPN system. In order to apply Holly et al.'s method<sup>7</sup> for determination of GP of the cross-linking component in an IPN system, however, we should know limitations of the self-similar behavior or any other effects caused by the presence of a second component in the IPN system.

Only few systematic studies were performed to investigate the effects of addition of a second component on the self-similar behavior of CG.<sup>11,15</sup> Scanlan et al.<sup>11</sup> explored divinyl-terminated PDMS systems of two different prepolymer molecular weights  $M_w = 1 \times 10^4$  and  $M_w = 4 \times 10^4$ . Nonreacting PDMS with molecular weight of about  $1.1 \times 10^4$  was added as an inert second component to each prepolymer. It was found that the critical self-similar behavior can be observed in the entire frequency window between 0.5 and 50 rad/s at any concentration of the inert component. However,  $S$  and  $n$  depend on the composition. For both prepolymers,  $S$  monotonously decreases with increasing concentration of the inert component.  $n$  is not affected by adding some of the inert component; however, high concentrations of the inert component result in very soft critical gels with an unusual high value of  $n$ , close to the theoretical limit of  $n = 1$ . Muller et al.<sup>15</sup> at about the same time found that addition of an inert component of moderate  $M_w$  increased the  $n$  value in cross-linking poly(ethylene oxide) with isocyanate. In all cases, the systems seemed to be mixed on molecular level; i.e., phase separation phenomena were excluded from these experiments.

Gelation is somewhat more complicated for highly asymmetric semi-IPN systems in which the inert poly-

**Table 1. Molecular Characterization of Poly( $\epsilon$ -caprolactone) Diol and Poly(styrene-*co*-acrylonitrile) (SAN)**

material	$M_n$	$M_w/M_n$	functionality	AN cont. (wt %)
PCL	$6.6 \times 10^3$	1.89	1.98	
SAN	$4.4 \times 10^4$	1.92		23.2

mer component is of much higher molecular weight and of different chemical structure than the cross-linkable component. This induces the effects of entanglement and phase separation between the components on the critical self-similar behavior of rheology. We selected a model semi-IPN system comprising poly( $\epsilon$ -caprolactone) diol (PCL) as a cross-linkable component and poly(styrene-*co*-acrylonitrile) (SAN) as an inert component. PCL is a unique polymer that exhibits good miscibility with various polymers.<sup>22</sup> As for PCL/SAN blends, one can tailor the phase separation behavior from totally homogeneous to phase separated by changing its acrylonitrile content in SAN.<sup>23</sup>

The rheology of such asymmetric semi-IPNs is initially dominated by the highly entangled SAN, while the lower molecular weight PCL acts as a plasticizer. However, with increasing extent of reaction the PCL gains long range connectivity and takes over the rheology. The motion of the high molecular weight linear chains becomes restricted by the emerging PCL network. This will be studied in the following, with an emphasis on the rheological properties near the gel point.

## Experimental Conditions

**Materials and Their Characterization.** Poly( $\epsilon$ -caprolactone) diols (PCLs) (commercial polymers of Daicel Chemical) were end-linked with a three-functional cross-linker, IPDI-T1890 supplied by Huels AG (poly-IPDI), in the presence of poly(styrene-*co*-acrylonitrile) (SAN) provided by Daicel Chemical. The poly-IPDI is virtually an isocyanurate of diisocyanatoisophorone containing three free NCO groups per molecule. It is the same as studied previously by Izuka et al.<sup>16</sup> The manufacturer's information specifies the NCO content in the compound as 17.5% by weight, although this value is calculated at 18.3% for the trimer. The poly-IPDI is a solid with a melting point of 110 °C. It was used without further purification.

The PCLs were synthesized by means of ring-opening polymerization of  $\epsilon$ -caprolactone with diol as an initiator so that the ends of the molecules should consist of an OH group that can be utilized for further chemical cross-linking. However, small amounts of COOH are generated when contaminating water initiates the ring-opening polymerization of  $\epsilon$ -caprolactone, and the ester bond of PCL is hydrolyzed. These two groups were quantitatively analyzed by titration and number average molecular weight, and a functionality of 1.98 was calculated based on these values.

SAN was synthesized at Daicel by means of radical polymerization. GPC measurement and nitrogen analysis were performed to determine molecular weight and acrylonitrile content, respectively. The SAN is polydisperse with  $M_w/M_n$  of approximately 2, and it contains 23.2 wt % of acrylonitrile. The characteristics of the polymeric component are summarized in Table 1.

The rheological properties of the two polymers differ greatly, as shown in Figure 1, mainly because of the difference of their molecular weights and glass transition temperatures. SAN at 140 °C exhibits the typical flow and entanglement behavior of a high molecular weight polymer. In the same frequency window, only the flow region could be observed for PCL because its molecular weight is below the critical molecular weight for entanglement.<sup>16</sup>

Drying at 100 °C for 14 h in vacuum was necessary to remove traces of low molecular weight derivatives and water from the components before mixing. Five PCL/SAN blend compositions without the cross-linker were prepared by solu-

Table 2. Composition of Blend Samples<sup>a</sup>

sample	FM100	FM95	FM90	FM80	FM70	FM60
PCL/SAN/poly-IPDI (wt/wt/wt)	93.6/0/6.4	88.9/5/6.1	84.2/10/5.8	74.9/20/5.1	65.5/30/4.5	56.1/40/3.9

<sup>a</sup> The number next to FM denotes the weight percent of cross-linking component.

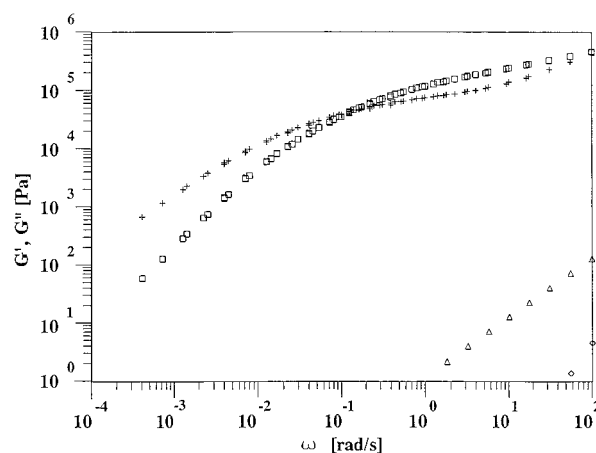


**Figure 1.** Dynamic storage  $G'$  and loss  $G''$  modulus of the materials are plotted against frequency  $\omega$ .  $G'$  ( $\square$ ) and  $G''$  ( $+$ ) of SAN were measured at 140, 150, 160, 170, and 180 °C and superposed with a reference temperature of 140 °C.  $G'$  ( $\diamond$ ) and  $G''$  ( $\Delta$ ) of PCL were measured at 140 °C.

tion casting from 40 wt % polymer solutions in dried dichloromethane. The solvent was evaporated in a hood at room temperature for 7 days and then in a vacuum oven in 2 days at 100 °C.

Stoichiometrically balanced mixtures of PCL/SAN/poly-IPDI (see Table 2) were prepared for each blend by adding a 60 wt % solution of the poly-IPDI in dried dichloromethane. The stoichiometric ratio,  $r$ , of the system is defined here as the initial molar ratio of isocyanate group to hydroxy group,  $[\text{NCO}]/[\text{OH}]$ , so that the concentration of poly-IPDI in the blends depended on concentration of PCL. For calculation of composition, we used the NCO content in the poly-IPDI of 17.5% by weight and the OH value of each PCL determined by the titration. Each mixture was stirred thoroughly at 80 °C for 5 min. The homogeneous mixture was then dried at 100 °C in vacuum for 10 min to remove the solvent, cooled to room temperature, and transferred into the rheometer.

**Rheological Experiments.** Oscillatory shear measurements in a Rheometrics dynamic mechanical spectrometer used parallel plates at a maximum strain amplitude of 10%. All samples were reacted isothermally at 110 °C under a dried air atmosphere. The evolution of the dynamic modulus during cross-linking was measured over a span of three decades of frequency between 0.1 and 100 rad/s by consecutive frequency scans. Each scan took less than 5 min. The mechanical properties were interpolated to determine the state at which  $\tan \delta$  is constant at low frequencies.

**Fully cross-linked samples** were prepared from the same mixtures as were used for the gelation studies. After the samples cured in the rheometer at 130 °C for 14 h, we confirmed that the dynamic moduli did not change anymore and that the samples had reached their highest possible degree of cross-linking.

**$T_g$  measurements** of the premixtures and the fully cross-linked samples were performed in a Perkin-Elmer DSC-2C under a nitrogen atmosphere with a heating rate of 20 K/min from 150 to 430 K. Each sample in its aluminum DSC pan was kept in a vacuum oven at 100 °C for at least 1 h to melt the PCL crystals, then it was quenched into liquid nitrogen (in an attempt to suppress crystallization of the PCL) and quickly transferred into the DSC. The glass transition temperature,  $T_g$ , reported here was chosen as the midpoint of the secondary transition in the DSC trace.

## Results

**Properties of Premixtures.** The complex dynamic viscosity,  $\eta^*$ , of the PCL/SAN blend samples was

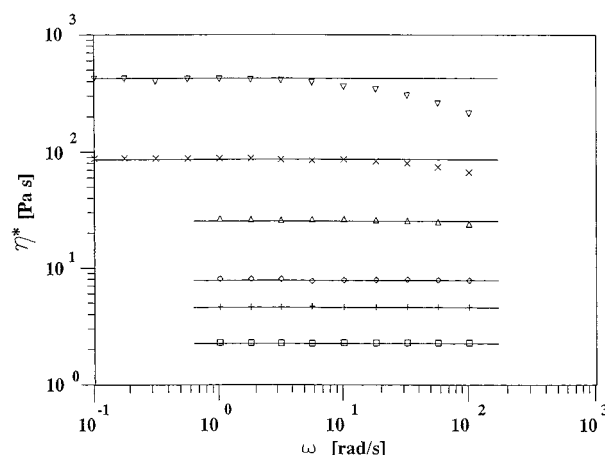


**Figure 2.** Complex dynamic viscosities  $\eta^*$  of the mixed precursors FM100 ( $\square$ ), FM95 ( $+$ ), FM90 ( $\diamond$ ), FM80 ( $\Delta$ ), FM70 ( $\times$ ), and FM60 ( $\nabla$ ) at 110 °C are plotted against frequency  $\omega$ . The low-frequency limit gives the zero shear viscosity  $\eta_p$  of the precursors.

measured at 110 °C with frequencies between 0.1 and 100 rad/s before addition of poly-IPDI, as shown in Figure 2. The onset of shear thinning, which is typical for high molecular weight polymers, was visible for the systems with high concentrations of SAN (FM60, FM70, FM80; the number next to FM denotes the weight percent of cross-linking component). The zero shear viscosity,  $\eta_0$ , was determined as the complex dynamic viscosity where it levels off at low frequencies.

DSC heating traces (Figure 3) suggested that PCL contained a small amount of crystal phase even after rapid quenching. The melting point of the crystal phase was 325 K, and the  $T_g$  of the amorphous phase was 212 K. SAN is an amorphous polymer with a  $T_g$  of 380 K. During heating, the PCL started to crystallize (DSC exotherm) and then it melted again (DSC endotherm). No significant transition was observed after the melting of the PCL crystal.

**Properties of Fully Cross-Linked Samples.** The dynamic complex moduli,  $G^*$ , of fully cross-linked samples with low SAN concentration (FM100, FM95, FM90 and FM80) were almost independent of frequency, as shown for 110 °C in Figure 4. For further evaluation of these systems, we adopted the value of  $G^*$  measured at  $\omega = 0.1$  rad/s as the equilibrium modulus,  $G_e$ . As far as FM70 and FM60,  $G^*$  depended on frequency and  $G_e$  could not be reduced to a single number.

The cross-linking reduces the crystallinity in the quenched samples. This can be seen when comparing the top curves in Figures 3 and 5. The addition of SAN further reduces the degree of crystallization in the PCL. This shows as endotherm in Figure 5. Up to an SAN concentration of 20 wt % (FM80) crystallinity can be detected in the quenched samples. For higher SAN content (FM70 and FM60) it seems to be suppressed completely.

The cross-linking of the PCL (FM100, FM95, FM90, FM80) increased the (single) glass transition temperature (see Figure 5). After cross-linking, FM70 and FM60 exhibited two glass transitions.  $T_g$ 's at low temperature did not increase significantly or were even lowered by the cross-linking. The higher  $T_g$ 's observed

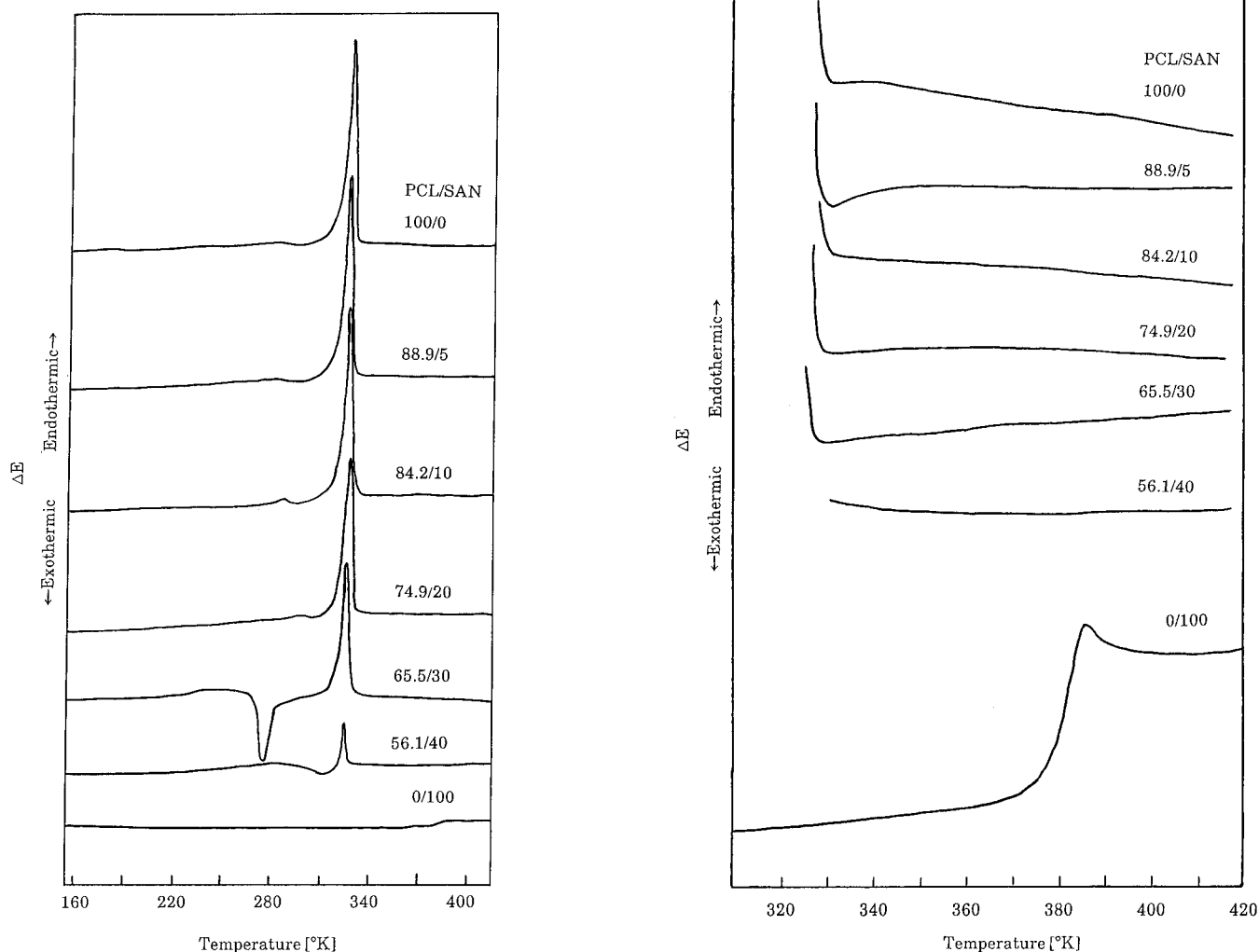


**Figure 3.** DSC traces of PCL/SAN blend systems before cross-linking (a) and its close up of the high-temperature region (b).

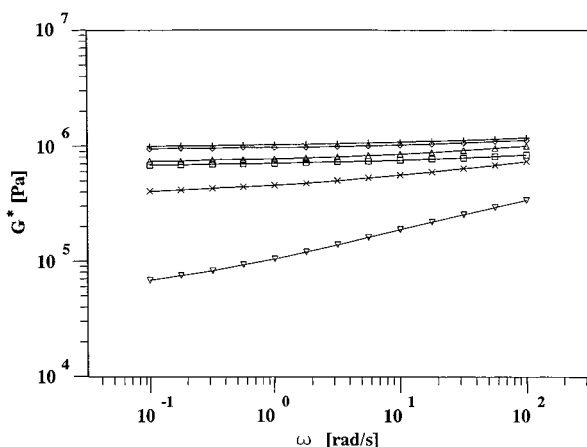


**Figure 4.** Complex dynamic moduli  $G^*$  of the fully cross-linked samples of FM100 ( $\square$ ), FM95 ( $+$ ), FM90 ( $\diamond$ ), FM80 ( $\triangle$ ), FM70 ( $\times$ ), and FM60 ( $\nabla$ ) at 110 °C are plotted against frequency  $\omega$ .

for FM70 and FM60 were 379 and 380 K, respectively. They were slightly lower than the  $T_g$  of SAN, which was determined to be about 380 K.

**Properties of Critical Gels.** At the beginning of the rheological measurement, before cross-linking starts, the system has very low values of  $G'$  and  $G''$ . With continuing cross-linking reaction, the values gradually increased and finally  $G'$  exceeded  $G''$ . This is shown in Figure 6 for FM80. In the course, the  $\tan \delta$  decreases

with reaction time, as shown in Figure 7 with the frequency as a parameter. The  $\tan \delta$  at low frequencies (between 0.1 and 10 rad/s) intersected at a certain time,  $t_c$ , which we will identify as gel point. For FM80,  $t_c$  was found to be about 111 min. Although  $t_c$  increased with increasing concentration of SAN, similar results were obtained for the other systems as long as the concentration of SAN was low enough (FM100, FM95, FM90, and FM70). However, such an instant at which  $\tan \delta$  became independent of frequency was not observed for FM60 in the accessible frequency window; i.e., the data gave no information about a possible GP.

Although  $G'$  and  $G''$  at  $t_c$  seem to exhibit the self-similar behavior in about the entire experimental frequency range (see Figure 8), small deviations start to occur at about 10 rad/s for all the systems. This can be seen more readily on a plot of  $\tan \delta$  (Figure 9). An exception is FM100, which exhibited the self-similar behavior in the entire frequency range of the experiment.

$S$  and  $n$  according to eqs 3 and 4 could be determined at  $t_c$  for these systems containing 30 wt % of SAN or less, as summarized Table 3. The relaxation exponent took on a range of values between about  $0.41 \leq n \leq 0.61$ . The corresponding gel stiffness values ranged from about  $3.6 \times 10^2$  (Pa s<sup>0.61</sup>) to  $1.1 \times 10^4$  (Pa s<sup>0.41</sup>). Figure 10 shows the relaxation exponent and the gel stiffness for the range of SAN content of our experiments. The exponent decreases with increasing SAN content, while

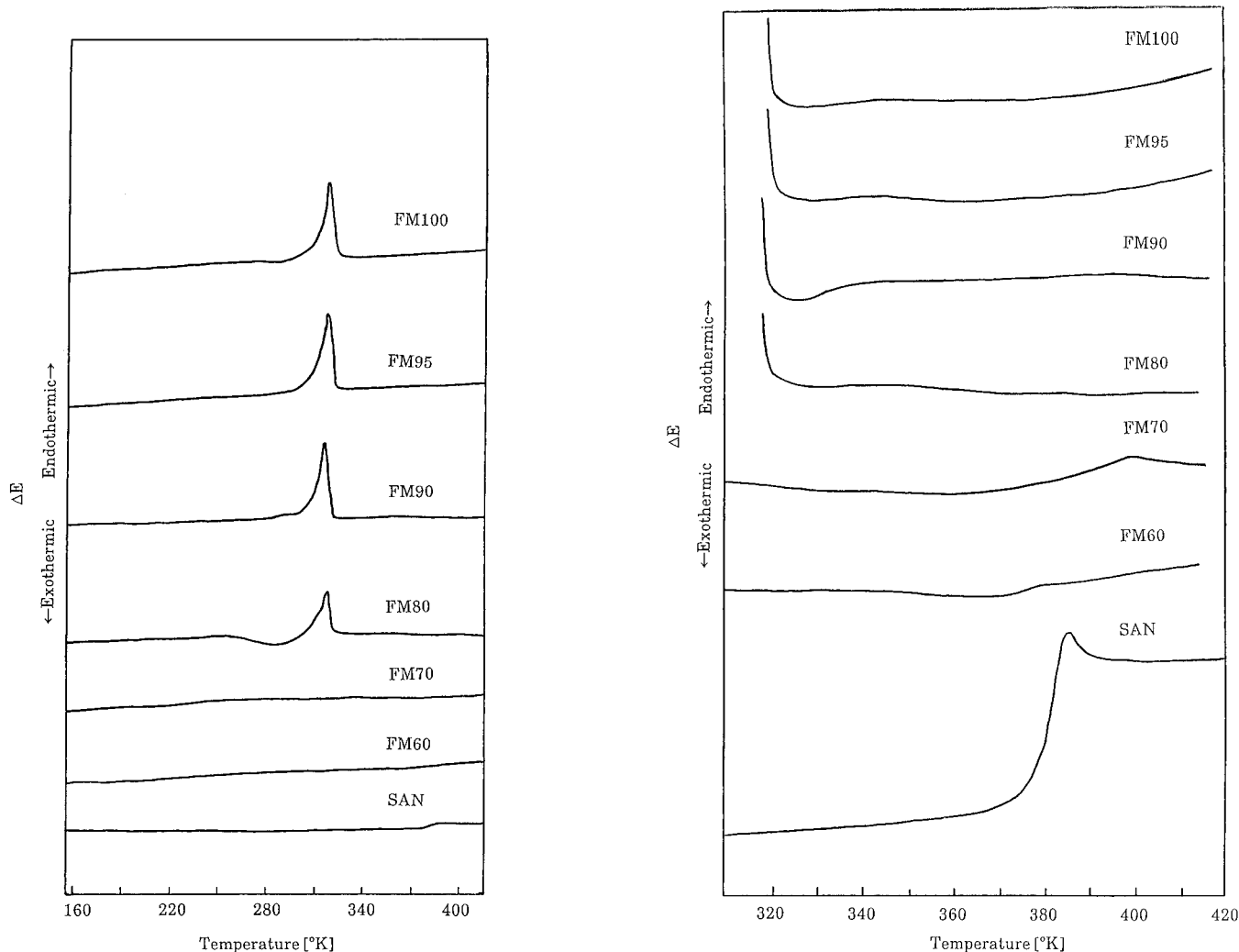


**Figure 5.** DSC traces of PCL/SAN blend systems after cross-linking (a) and its close up of high-temperature region (b).

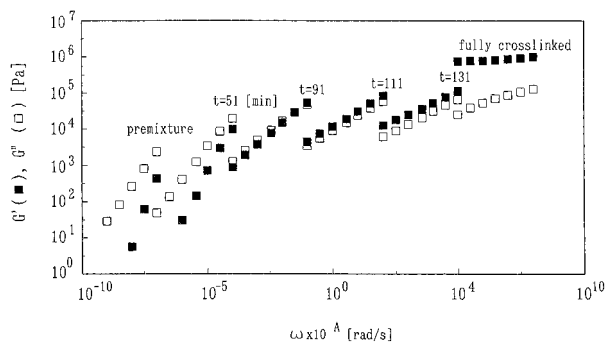


**Figure 6.** Dynamic storage  $G'$  (■) and loss  $G''$  (□) moduli for the premixture of FM80, FM80 during the isothermal cross-linking reaction at 110 °C and the fully cross-linked FM80 plotted against frequency  $\omega$ . The temperature was 110 °C. The curves were horizontally shifted by the factors,  $A = -9$  for the premixture,  $A = -6$  for  $t = 51$  min,  $A = -3$  for  $t = 91$  min,  $A = 0$  for  $t = 111$  min,  $A = 3$  for  $t = 131$  min, and  $A = 6$  for the fully cross-linked, in order to avoid overlap.

$S$  increases with increasing SAN content for these samples except for FM70. The exponent of FM70 is between those of FM95 and FM90, and the gel stiffness is slightly smaller than that of FM80.

## Discussion

### Phase Separation Induced by Cross-Linking.

With continuing cross-linking reaction, the cross-linking component of the semi-IPN system increases its molec-

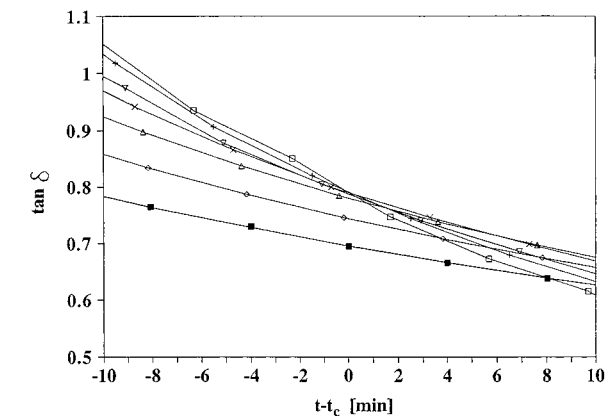


**Figure 7.** Evolution of  $\tan \delta$  of FM80 during the isothermal cross-linking reaction at 110 °C with frequency of 0.1 (rad/s) (□), 0.3162 (+), 1 (▽), 3.162 (×), 10 (△), 31.62 (◇), and 100 (■). The maximum strain amplitude was 10%.

ular weight and forms a network structure. The increase of the molecular weight reduces the gain of entropy of mixing. In addition, the network structure has to store the strain energy induced by swelling with a linear component. Since these additional energies make the homogeneous state unstable, molecularly mixed components before cross-linking might phase separate in the course of cross-linking.<sup>3</sup> The increase of the molecular weight also changes the shape of the coexistence curve of the phase diagram. For linear chains of uniform molecular weights  $M_A$  and  $M_B$ , the

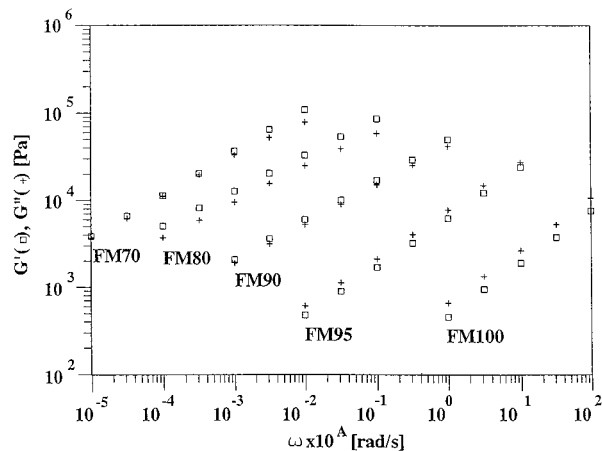


**Figure 8.** Dynamic storage  $G'$  (□) and loss  $G''$  (+) moduli for the PCL/SAN blends at critical state plotted against frequency  $\omega$ . The temperature was 110 °C, and the maximum strain amplitude was 10%. The curves were horizontally shifted by the factors,  $A = 0$  for FM100,  $A = -1$  for FM95,  $A = -2$  for FM90,  $A = -3$  for FM80, and  $A = -4$  for FM70, in order to avoid overlap.

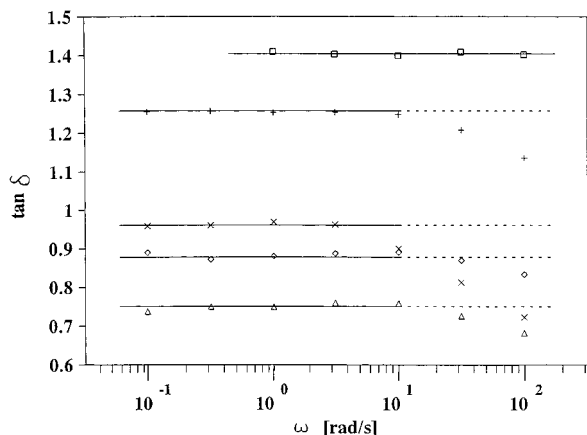


**Figure 9.**  $\tan \delta$  at the critical state plotted against frequency  $\omega$  for FM100 (□), FM95 (+), FM90 (◇), FM80 (Δ), and FM70 (×). All lines are parallel to the horizontal axis.

**Table 3. Relaxation Exponent  $n$  and the Gel Stiffness  $S$  of SAN/PCL Blends at Critical State**

sample	FM100	FM95	FM90	FM80	FM70	FM60
$n$	0.61	0.57	0.46	0.41	0.49	
$S$ (Pa s <sup>n</sup> )	$3.6 \times 10^2$	$1.3 \times 10^3$	$4.9 \times 10^3$	$1.1 \times 10^4$	$9.1 \times 10^3$	

critical composition,  $\Phi_c$ , can be expressed as

$$\Phi_c = \frac{\sqrt{N_B}}{\sqrt{N_A} + \sqrt{N_B}} \quad (5)$$

where  $N_A$  and  $N_B$  are the degree of polymerization of components A and B, respectively.<sup>24</sup> Even if the above equation has been derived for linear molecules, it gives guidance for the system here where the chains of component A are highly branched and broadly distributed in size due to cross-linking. With an increase of the molecular weight of one of the components, the phase diagram becomes asymmetric. At the extreme of  $N_A \rightarrow \infty$ ,  $\Phi_c$  goes toward 0, suggesting that one of the phase-separated phases consists of its pure component.

The DSC results before cross-linking suggest that the PCL/SAN blends consist of crystalline PCL and an amorphous phase consisting of molecularly mixed PCL and SAN at temperatures below the crystal melting

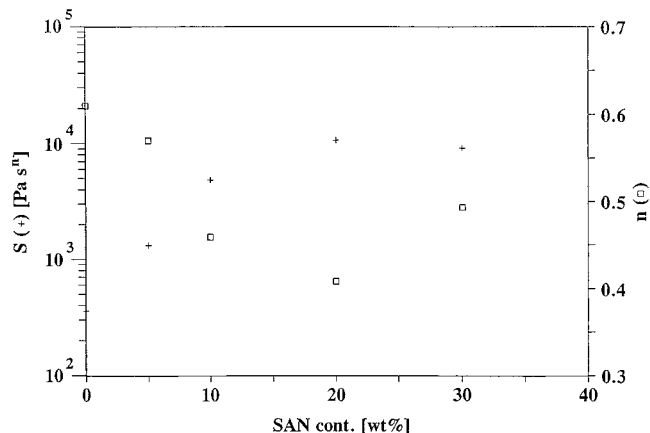


**Figure 10.** Gel stiffness  $S$  (+) and relaxation exponent  $n$  (□) plotted against SAN content.

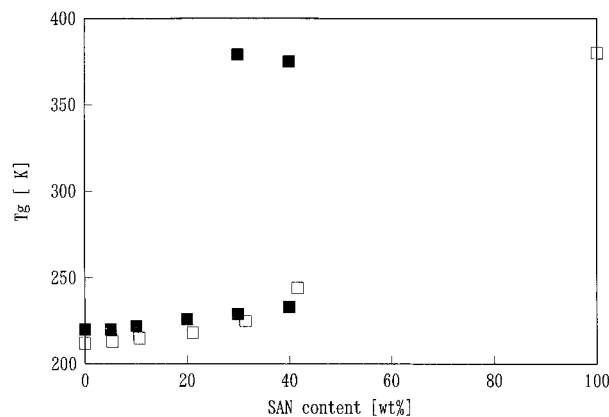


**Figure 11.** Glass transition temperature  $T_g$  of the PCL/SAN blend system before (□) and after cross-linking (■) plotted against SAN content.

point of PCL. Since a single  $T_g$  was observed for each un-cross-linked blend and the  $T_g$  monotonically increased with increasing SAN content (see Figure 11), the system is supposed to be in its homogenous state at the cross-linking temperature of 110 °C.

After completion of the cross-linking reaction, FM70 and FM60 exhibit two  $T_g$ 's. As the asymmetric phase diagram of phase-separated semi-IPN suggests, the higher ones were almost equal to the  $T_g$  of SAN itself and the change of heat capacity at  $T_g$  was very small. The lower ones are slightly higher than the  $T_g$  of cross-linked PCL. From these results, we may conclude that the systems phase separated into an almost pure SAN phase and a PCL rich phase containing some amount of SAN. However, we could not determine whether such transition from the homogeneous state to the partially phase separated state took place before or after GP of PCL. For cross-linked FM95, FM90, and FM80, there is no evidence for such phase separation.

**Detection of GP in a Semi-IPN System.** Theories of gelation<sup>25,26</sup> predict a power law cluster number distribution at the gel point in terms of the cluster mass,  $M$

$$N_M \sim M^{-\gamma} \quad (6)$$

where  $\gamma$  is termed the polydispersity index. The cluster radius distribution is also expected to be a power law at GP

$$R_M \sim M^{d_f/d_f} \quad (7)$$

where  $d_f$  is the fractal dimension. The self-similar

relaxation behavior of CG might originate from these statistical self-similarities. Several researchers<sup>13,17,27</sup> derived expressions of the relaxation exponent in terms of the fractal dimension by assuming that  $N_M$  and  $M$  independently relate to the spectrum  $H(\lambda)$ . A critical gel consisting of only cross-linkable component satisfies those eqs over a very wide range of mass. This leads to a very wide time range where the self-similar relaxation behavior can be observed.

If we add to CG a linear polymer that does not satisfy eq 6, the power law cluster number distribution can be observed only at high molecular weights, above the molecular weight of the linear component. This explains the restricted time window of the self-similar relaxation behavior in a semi-IPN system containing long linear molecules.

In fact, we found that the lower limiting relaxation time,  $\lambda_0$ , has values in the experimental frequency range for FML95, FM90, FM80, and FM70. In comparison, the  $\lambda_0$  of FM100, which does not contain SAN, is outside of the accessible frequency range. We should, however, emphasize here that the self-similar relaxation behavior can be observed at low frequencies for these systems. This suggests that these systems at their gel point still possess the typical self-similarity if we probe spatial sizes larger than the size of the SAN molecule. Therefore, the observed  $t_c$  is considered to be the gel time of PCL.

For the premixtures, shear thinning was observed only for FM80, FM70, and FM60 and occurred at particular frequencies, depending on the composition (see Figure 2). However,  $\omega_0 = 1/\lambda_0$  is observed even for FM95 and FM90 and does not seem to depend on the composition very much (see Figure 9). This might be explained as follows: The transition of relaxation behavior from entanglement to flow region is an expression of the longest relaxation time of SAN. This depends on the composition since PCL acts as a diluent of SAN in the premixtures.

The DSC results suggest that phase separation induced by cross-linking takes place in FM70 and FM60. Only for FM60, however, could the self-similar relaxation behavior not be observed. This suggests that the phase separation may already start before the FM60 reaches GP. If the phase separation takes place before GP, we would not expect the self-similar behavior within our experimental frequency window. The phase separation might affect the self-similar behavior of FM70 as well. This would explain its peculiar set of  $n$  and  $S$  values that deviate from the tendency observed on the samples with low SAN concentration. A careful investigation of the above hypothesis would require measurements of the structure growth during cross-linking, possibly by light scattering.

In the next two sections, we will discuss the values of  $S$  and  $n$  that were determined for the system with low concentrations of SAN (FM100, FM95, FM90, and FM80).

**Effect of Addition of Linear Polymer on the Relaxation Exponent.** This study shows remarkable contrast to Scanlan's observation who found that  $S$  decreases and  $n$  increases with increasing concentration of the nonreacting linear polymer. This might be attributed to the difference of molecular weights of the additives. In the case of Scanlan's PDMS system, the molecular weight of the un-cross-linkable PDMS is below the entanglement molecular weight of about 24 500.<sup>28</sup> Therefore, the PDMS acts as a diluent in the system. On the other hand, the molecular weight of SAN in this study is much above the entanglement

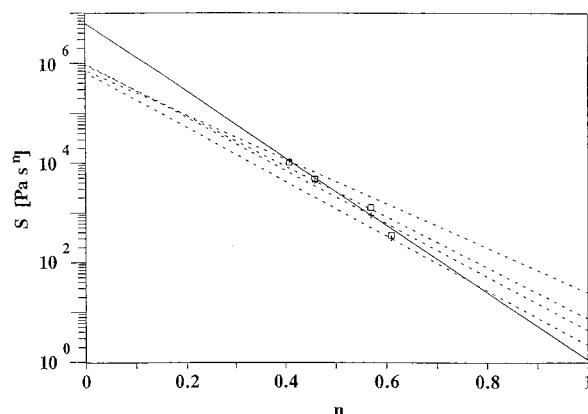


**Figure 12.** Experimental values ( $\square$ ) and calculated values ( $+$ ) of the gel stiffness  $S$  plotted against the relaxation exponent  $n$ . A solid line is obtained from a least-squares fit of eq 10 with the experimental values. Each broken line connected the equilibrium modulus  $G_e$  and zero shear viscosity  $\eta_p$  of each precursor blend.

molecular weight, which was reported to be 11 000 for SAN with 24.1 wt % of acrylonitrile.<sup>29</sup> Therefore, the dilution effect is masked by the entanglement behavior of the high molecular weight SAN. Molecular weight of a linear component might be an important factor that determines whether  $n$  increases or decreases with increasing concentration of linear component.

Durand et al.<sup>13</sup> and Martin et al.<sup>17</sup> predicted  $n$  in terms of the fractal dimension as

$$n = \frac{d}{d_f + 2} \quad (8)$$

where  $d$  is the space dimension ( $=3$ ). Muthukumar<sup>27</sup> considered the excluded volume effect and suggested that, if the excluded volume effect is fully screened, the relaxation exponent becomes

$$n = \frac{d(d + 2 - 2d_f)}{2(d + 2 - d_f)} \quad (9)$$

These equations suggest that the relaxation exponent increases with decreasing fractal dimension. Our observation, therefore, can be qualitatively elucidated: As the SAN concentration is increased, the structure becomes more dense and  $d_f$  is higher, leading to a decrease in  $n$ .

**Relationships between  $S$  and  $n$ .** Many observations indicated that  $S$  and  $n$  are coupled. Because of its physical dimension of  $\text{Pa s}^n$ , it was apparent that the stiffness  $S$  of the critical gel was composed of a modulus and a time constant.<sup>8</sup> An experimental relationship between  $S$  and  $n$  was found for cross-linking PDMS systems<sup>11</sup> as

$$S = G_{cg} \lambda_{cg}^n \quad (10)$$

where the meaning of the modulus  $G_{cg}$  and the time constant  $\lambda_{cg}$  (subscript cg for critical gel) needs to be specified. It was not completely clear how this relation can be extended to semi-IPNs or whether it is applicable at all. This was examined by plotting  $\log S$  against  $n$  (see Figure 12). In fact, we can observe fairly good linearity between  $n$  and  $\log S$ . A least-squares fit (a solid line) would give  $G_{cg} = 6.31 \times 10^6 \text{ Pa}$  and  $\lambda_{cg} = 1.90 \times 10^{-8} \text{ s}$ .

It was found that  $G_{cg}$  was very close to the modulus of the fully cross-linked material,  $G_e$ .<sup>11</sup> The most simple

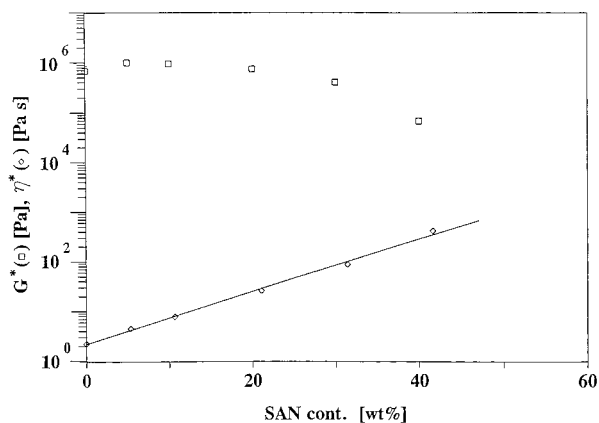


**Figure 13.** Complex dynamic viscosities  $\eta^*$  (+) of the mixed precursors and the complex dynamic moduli  $G^*$  ( $\square$ ) of the fully cross-linked materials plotted against SAN content. The data were taken at  $\omega = 0.1$  rad/s. A straight line for the viscosities is obtained from a least-squares fit.

assumptions for  $\lambda_{cg}$  were that it is either the low-frequency end of the power law, as defined in eqs 1–3, the longest relaxation time of the precursor, or the ratio of precursor viscosity and modulus,  $\eta_p/G_e$ .<sup>11</sup> The vastly different relaxation time scales of the two components in our system allow us to further explore the meaning of  $\lambda_{cg}$ .

Recently, the relationship  $\lambda_{cg} = \eta_p/G_e$  was investigated<sup>16</sup> in detail for PCL systems with different molecular weight precursors. It was found that the relationship between  $S$  and  $n$  can be represented approximately in terms of  $G_e$  and  $\eta_p$  as

$$S = G_e(\eta_p/G_e)^n \quad (11)$$

where the two parameters are functions of molecular weight.  $S$  values according to eq 11 were calculated by using experimentally determined values of  $n$ ,  $G_e$ , and  $\eta_p$  for each system (see Figure 13). The calculated values (crosses on broken lines) are shown in comparison with the corresponding experimental  $S$  values (squares) in Figure 12, as well. There are only small discrepancies between the calculated values and the experimental values. We may conclude that eq 11 is a reasonably good expression for the relationship between  $S$  and  $n$ , which is applicable even for the systems containing a long linear component.

Scanlan et al.'s<sup>11</sup> other two assumptions for  $\lambda_{cg}$  do not seem to apply to these semi-IPN systems, where the crossover time  $\lambda_0 (=1/\omega_0)$  is of the order of  $10^{-1}$  (see Figure 9). The longest relaxation time of the precursor,  $\lambda_p$ , is of the same order as  $\lambda_0$  and, hence, is also much larger than  $\lambda_{cg}$ . In such a case, it is concluded that eq 10 cannot predict the value  $\lambda_0$ .

## Conclusions

These results suggest that the gel point of a cross-linking component in a semi-IPN system is detectable by its self-similar relaxation behavior, as long as the system is homogeneous. From a practical point of view, this method is advantageous because it is simpler than conventional methods and allows simultaneous measurement during processing.

The self-similar relaxation behavior is observed in cross-linking poly( $\epsilon$ -caprolactone) and poly(styrene-co-acrylonitrile) blends with low concentrations of the linear component from the restricted time window. Phase separation might hinder the self-similar behavior

for the systems with a high concentration of the linear component.

The relaxation properties,  $n$  and  $S$ , strongly depend on composition. The relaxation exponent decreases with increasing concentration of the linear component, suggesting that the fractal dimension increases with increasing concentration of the linear component. The molecular weight of the nonreacting linear component might be an important factor that determines whether  $n$  increases or decreases with increasing concentration of the linear component.

An experimental relationship between  $n$  and  $S$ ,  $S = G_e(\eta_p/G_e)^n$ , is observed in this system as was observed in 100% poly( $\epsilon$ -caprolactone) critical gels. Here,  $\eta_p$  is the zero shear viscosity of the mixture at the onset of the cross-linking reaction and  $G_e$  is the final modulus.

**Acknowledgment.** We gratefully acknowledge Daicel Chemical Industries, Ltd. for financial support and providing samples. We also thank Huels AG for samples of the cross-linker.

## References and Notes

- (1) Sperling, L. H. *Interpenetrating Polymer Networks and Related Materials*; Plenum Press: New York, 1981.
- (2) Tran-Cong, Q.; Nagai, T.; Nakagawa, T.; Yano, O.; Soen, T. *Macromolecules* **1981**, *22*, 2720.
- (3) Bauer, B. J.; Briber, R. M.; Han, C. C. *Macromolecules* **1989**, *22*, 940.
- (4) Yamakawa, K.; Takagi, Y.; Inoue, T. *Polymer* **1989**, *60*, 1839.
- (5) Binder, K.; Frisch, H. L. *J. Chem. Phys.* **1984**, *81*, 15.
- (6) Onuki, A. *Phys. Rev.* **1988**, *A38*, 2192.
- (7) Holly, E. E.; Venkataraman, S. K.; Chambon, F.; Winter, H. H. *J. Non-Newtonian Fluid Mech.* **1988**, *27*, 17.
- (8) Chambon, F.; Winter, H. H. *Polym. Bull. (Berlin)* **1985**, *13*, 499.
- (9) Chambon, F.; Winter, H. H. *J. Rheol.* **1987**, *31*, 683.
- (10) Winter, H. H.; Chambon, F. *J. Rheol.* **1986**, *30*, 367.
- (11) Scanlan, J. C.; Winter, H. H. *Macromolecules* **1991**, *24*, 47.
- (12) Chambon, F.; Petrovic, Z. S.; MacKnight, W. J.; Winter, H. H. *Macromolecules* **1986**, *19*, 2146.
- (13) Durand, D.; Delsanti, M.; Adam, M.; Luck, J. M. *Europhys. Lett.* **1987**, *3*, 97.
- (14) Winter, H. H.; Morganelli, P.; Chambon, F. *Macromolecules* **1988**, *21*, 532.
- (15) Muller, R.; Gerard, E.; Dugand, P.; Rempp, P.; Gnanou, Y. *Macromolecules* **1991**, *24*, 1321.
- (16) Izuka, A.; Winter, H. H.; Hashimoto, T. *Macromolecules* **1992**, *25*, 2422.
- (17) Martin, J. E.; Adolf, D.; Wilcoxon, J. P. *Phys. Rev.* **1989**, *A39*, 1325.
- (18) Takahashi, M.; Yokoyama, K.; Masuda, T. *J. Chem. Phys.* **1994**, *101*, 798.
- (19) Nijenhuis, K.; Winter, H. H. *Macromolecules* **1989**, *22*, 411.
- (20) Lin, Y. G.; Mallin, D. T.; Chien, J. C.; Winter, H. H. *Macromolecules* **1991**, *24*, 47.
- (21) Winter, H. H.; Izuka, A.; De Rosa, M. E. *Polym. Gels Networks* **1994**, *2*, 339–345.
- (22) Robeson, L. M. *Polym. Eng. Sci.* **1984**, *24*, 587.
- (23) Chiu, Sc.; Smith, T. G. *J. Appl. Polym. Sci.* **1984**, *29*, 1797.
- (24) Koningsveld, R.; Staverman, A. J. *J. Polym. Sci., Polym. Phys. Ed.* **1968**, *6*, 325.
- (25) Stauffer, D.; Coniglio, A.; Adam, M. *Adv. Polym. Sci.* **1982**, *44*, 103.
- (26) Schosseler, F.; Leibler, L. *J. Phys. Lett.* **1984**, *45*, 1501.
- (27) Muthukumar, M. *Macromolecules* **1989**, *22*, 4656.
- (28) Ferry, J. D. *Viscoelastic Properties of Polymers*; John Wiley and Son: New York, 1980.
- (29) Wu, S. *Polymer* **1987**, *28*, 1144.